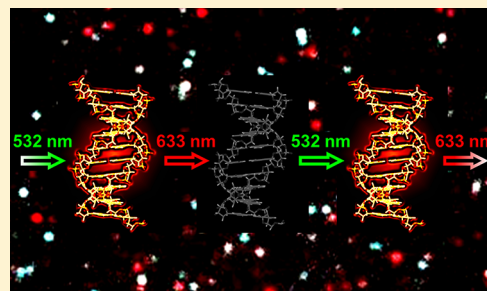


# Reversible Fluorescence Photoswitching in DNA

Darren A. Smith,<sup>†</sup> Philipp Holliger,<sup>‡</sup> and Cristina Flors<sup>\*,†,§</sup><sup>†</sup>EaStChem School of Chemistry, University of Edinburgh, Joseph Black Building, The King's Buildings, West Mains Rd, Edinburgh EH9 3JJ, United Kingdom<sup>‡</sup>MRC Laboratory of Molecular Biology, Hills Road, Cambridge CB2 0QH, United Kingdom<sup>§</sup>IMDEA Nanociencia, Calle Faraday 9, Ciudad Universitaria de Cantoblanco, 28049 Madrid, Spain

## Supporting Information

**ABSTRACT:** We describe the engineering of reversible fluorescence photoswitching in DNA with high-density substitution, and its applications in advanced fluorescence microscopy methods. High-density labeling of DNA with cyanine dyes can be achieved by polymerase chain reaction using a modified DNA polymerase that has been evolved to efficiently incorporate Cy3- and Cy5-labeled cytosine base analogues into double-stranded DNA. The resulting biopolymer, "CyDNA", displays hundreds of fluorophores per DNA strand and is strongly colored and highly fluorescent, although previous observations suggest that fluorescence quenching at such high density might be a concern, especially for Cy5. Herein, we first investigate the mechanisms of fluorescence quenching in CyDNA and we suggest that two different mechanisms, aggregate formation and resonance energy transfer, are responsible for fluorescence quenching at high labeling densities. Moreover, we have been able to re-engineer CyDNA into a reversible fluorescence photoswitchable biopolymer by using the properties of the Cy3–Cy5 pair. This novel biopolymer constitutes a new class of photoactive DNA-based nanomaterial and is of great interest for advanced microscopy applications. We show that reversible fluorescence photoswitching in CyDNA can be exploited in optical lock-in detection imaging. It also lays the foundations for improved and sequence-specific super-resolution fluorescence microscopy of DNA.



## INTRODUCTION

Fluorescence photoswitching constitutes the core of new and powerful imaging techniques that are able to greatly improve spatial resolution in fluorescence microscopy. These "super-resolution" techniques use different illumination strategies to control the fluorescence of photoswitchable molecules, allowing an improvement of spatial resolution that goes beyond the diffraction limit of light.<sup>1</sup> Recent advances in fluorescence photoswitching have been driven by the dramatic expansion of super-resolution microscopy,<sup>2–4</sup> and have also impacted the development of techniques such as optical lock-in detection (OLID) imaging.<sup>5,6</sup> OLID imaging uses fluorescence photoswitching to improve image contrast, instead of spatial resolution, in fluorescence microscopy by modulating the fluorescence emission through optical control. Subsequent cross-correlation analysis with a reference waveform isolates the modulated signal of interest from the unmodulated background signal.

To fully realize the great potential of these advanced imaging methods, novel strategies to label cell components with photoswitchable fluorophores in high density are needed. High-density labeling is crucial for super-resolution microscopy, as labeling density directly affects the best achievable spatial resolution.<sup>7–9</sup> While many options exist to label proteins with photoswitchable fluorescent molecules, the choices for DNA are very limited.<sup>10</sup> So far, super-resolution imaging of DNA by

single-molecule localization has been possible by stochastic blinking or transient binding of dyes that can associate noncovalently to DNA,<sup>11–15</sup> as well as by click chemistry.<sup>16</sup>

Here we describe a strategy for reversible fluorescence photoswitching in DNA with high-density substitution and control over sequence. It was recently reported that high-density labeling of DNA with cyanine dyes can be achieved by polymerase chain reaction (PCR) using a modified DNA polymerase that has been evolved to efficiently incorporate the cytosine base analogues Cy3- and Cy5-dCTP (dCTP = 5-aminopropargyl-2'-deoxycytidine 5'-triphosphate) into double-stranded DNA.<sup>17</sup> The resulting biopolymer, termed "CyDNA", can be up to about 1.5 kbp long, and displays hundreds of fluorophores per DNA strand. CyDNA is strongly colored and highly fluorescent, although previous observations suggest that fluorescence quenching at such high density might be a concern, especially for Cy5.<sup>17</sup> Herein, we first investigate the mechanisms of fluorescence quenching in CyDNA. In addition, we show that CyDNA can be re-engineered to perform reversible fluorescence photoswitching by using the properties of the Cy3–Cy5 pair.<sup>18,19</sup> By bringing Cy3 and Cy5 into close contact in the presence of a thiol compound and in the absence

Received: June 11, 2012

Revised: August 2, 2012

Published: August 3, 2012

of oxygen, the pair acts as a fluorescence photoswitch that can be activated at 532 nm and deactivated at 633 nm. We have incorporated the Cy3–Cy5 pair into CyDNA using two different approaches, and we demonstrate the potential of this strategy in OLID and other advanced fluorescence microscopy methods for imaging of DNA with sequence specificity.

## RESULTS AND DISCUSSION

**Fluorescence Quenching in CyDNA.** In order to identify the sources of fluorescence quenching, steady-state spectroscopy was performed on Cy3- and Cy5-substituted CyDNA (hereafter Cy3DNA and Cy5DNA, respectively). Figure 1A

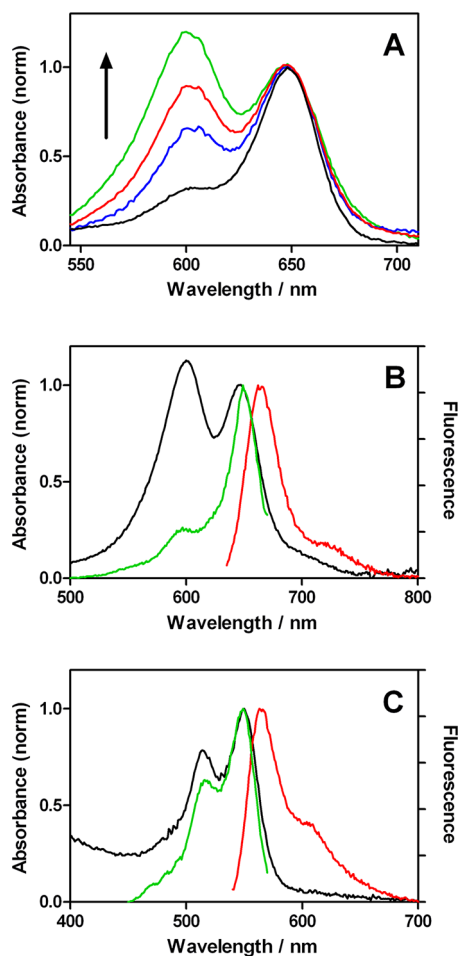


**Figure 1.** (A) Normalized absorption spectra of Cy5-dCTP (66 nM, black) and Cy5DNA at increasing labeling density (see Table S1 in the Supporting Information) in Tris-EDTA buffer (blue, red, green). The band at 600 nm strongly suggests the formation of H-aggregates at higher labeling densities. (B) Absorption (black), fluorescence emission (red), and excitation (green) of Cy5DNA at a maximum estimated labeling density of 25%. (C) Absorption (black), fluorescence emission (red), and excitation (green) of Cy3DNA at similar labeling density as (B).

shows the absorption spectra of 1.3 kbp fragments of CyDNA (50% GC content) with different Cy5 labeling densities, up to an estimated 25% labeled base pairs (see Table S1 and text in the Supporting Information for details). The most striking feature in these spectra is the band at about 600 nm, which increases concomitantly with the labeling density. This band is

blue-shifted with respect to the  $S_0 \rightarrow S_1$  band of Cy5 at 650 nm, and its excitation does not result in fluorescence emission, as seen in the excitation spectra of this species (Figure 1B). This observation suggests that the band at 600 nm can be ascribed to the presence of nonfluorescent H-aggregates.<sup>20</sup> An H-aggregate is a common dye–dye aggregate that can be described as a stacked dye dimer in parallel arrangement (distance between dyes of 3–5 Å), and whose formation is characterized by a decrease in the monomeric dye absorption band and an increase in a nonfluorescent, blue-shifted band.<sup>20</sup> There is also evidence for H-aggregate formation in Cy3DNA, although it is much less prominent than for Cy5DNA (Figure 1C). These aggregates are likely to be in the DNA major groove, which is thought to be the location of the dyes in CyDNA.<sup>17</sup> H-aggregate formation by these dyes has been observed previously in multiply labeled DNA,<sup>21</sup> polyelectrolytes<sup>22</sup> and antibodies,<sup>23</sup> and was also more pronounced for Cy5 than for Cy3.<sup>23</sup>

In addition to the formation of nonfluorescent aggregates, further steady-state fluorescence experiments point to the existence of another fluorescence quenching mechanism. Solutions of Cy5-dCTP monomer and Cy5DNA optically matched (i.e., equally absorbing) and excited at 644 nm (within the  $S_0 \rightarrow S_1$  absorption band), showed very different fluorescence intensity (Figure S1 in the Supporting Information). Quenching of Cy5DNA was 79% compared to free Cy5-dCTP, and 84% for Cy3DNA compared to Cy3-dCTP (excitation wavelength was 532 nm in the latter case). This additional quenching channel is likely due to resonance energy transfer (RET) or energy hopping between fluorophores, which may be trapped in low-energy nonemissive sites, as suggested before for densely labeled antibodies.<sup>23,24</sup> Due to the small residual absorption of the nonfluorescent H-aggregates at the excitation wavelengths, the contribution of other processes such as RET mentioned above might be slightly overestimated.

It is worth noting that besides the interaction between dyes attached to the same DNA strand, it is also possible to have interactions with dyes that are attached to the complementary strand. This results in a range of possible distances and angles, which in turn will be reflected in a range of coupling strengths and RET efficiencies. Moreover, the linker that connects the cytosine base with the dye is fairly long ( $C_5$ ), adding additional flexibility and modes of interaction.

**Engineering Reversible Fluorescence Photoswitching in CyDNA.** To introduce reversible fluorescence photoswitching in CyDNA, we took advantage of the switching properties of the Cy3–Cy5 pair.<sup>18,19</sup> As mentioned above, when Cy3 and Cy5 are closer than 3 nm and in the presence of a “switching buffer” (a thiol compound and an enzymatic oxygen scavenging system), the pair acts as a fluorescence photoswitch that can be activated at 532 nm and deactivated at 633 nm. The mechanism of fluorescence photoswitching involves the metastable formation of a dark Cy5-thiol adduct, although the role of Cy3 as an activator is still unclear.<sup>25</sup>

We introduced fluorescence photoswitching in CyDNA using two different strategies. In a first approach, we produced a Cy3–Cy5 heteroduplex CyDNA in which each strand was substituted by only one type of dye (Cy3/5DNA). In the other approach, we produced mixed CyDNA by randomly incorporating an equal mixture of Cy3 and Cy5 during PCR (Cy\*DNA). In both cases, 1.3 kbp fragments were produced, of which a maximum of 25% were labeled (see Supporting Information for more details). Figure 2 depicts the number of fluorescent molecules as a function of time, with 532 nm

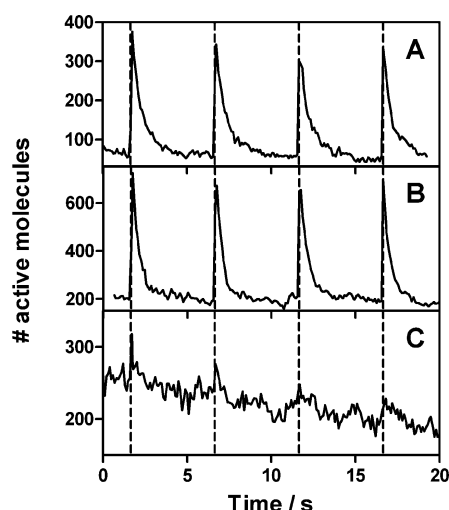


**Figure 2.** Fluorescence photoswitching of (A) Cy3/5DNA, (B) Cy\*DNA, and (C) Cy5DNA. The sample was immobilized onto a polylysine-coated coverglass and imaged in a chamber containing switching buffer. The molecules were continuously excited at 633 nm, and pulses of 532 nm were used to photoactivate fluorescence (represented by the dashed lines).

activation pulses every 5 s, and confirms that both strategies yielded samples that were able to photoswitch in a reliable and reversible manner (panels A and B). At least 20 photoswitching cycles could be achieved with no significant photobleaching (only about 30%). Fluorescence photoactivation of both types of CyDNA was much more efficient than pure Cy5DNA (Figure 2C), even though the fluorescence of the latter could be slightly activated with 532 nm pulses, consistent with previous observations.<sup>26</sup> Switching from the bright to the dark state was faster in Cy\*DNA, with an average rate constant of  $2.7 \text{ s}^{-1}$ , compared to  $1.5 \text{ s}^{-1}$  for Cy3/5DNA, suggesting that incorporating Cy5 in both strands increases the likelihood of interaction with thiols.

The trace in Figure 3A highlights the reliability of CyDNA photoswitching even at the single-molecule level, in contrast

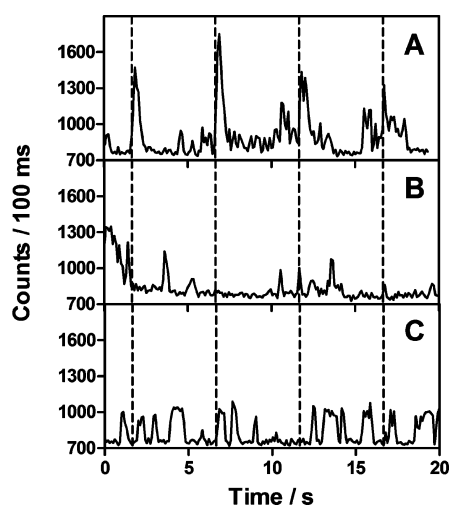


**Figure 3.** Single-molecule intensity traces with excitation at 633 nm and 532 nm photoactivation in switching buffer of (A) Cy3/5DNA, (B) Cy5DNA, and (C) Cy5-dCTP. Reliable photoswitching at the single-molecule level is clear in (A), in contrast to stochastic blinking in (B) and (C).

with the stochastic blinking of Cy5DNA and Cy5-dCTP (Figure 3, B and C, respectively). The fluorescence intensity values in highly substituted CyDNA compared to Cy5-dCTP monomers point once again to efficient fluorescence quenching, consistent with our data above.

**Reversible Fluorescence Photoswitching for Advanced Fluorescence Microscopy.** We have applied CyDNA photoswitching in proof-of-concept photoactivated localization microscopy (PALM) (Figure S2 in the Supporting Information), showing that the structure of a CyDNA fragment can be resolved. Moreover, the introduction of reliable and reversible fluorescence photoswitching in DNA (as opposed to stochastic photoblinking) opens up the possibility of performing OLID imaging on labeled DNA. As described above, OLID is a technique designed to enhance image contrast in fluorescence imaging, and necessarily needs controllable and reversible fluorescence photoswitching.

A mixture of Cy3/5DNA and Cy5DNA (2:1) was imaged at 633 nm and activated at 532 nm every 5 s (0.4 mW, 50 ms per pulse). Movies consisting of 200 frames were collected, and every pixel was compared to a reference waveform, which was generated from the average intensity of each frame in the movie. The resulting correlation image, with values ranging from 0 to 1, is shown in Figure 4A. Figure 4B shows the overlay

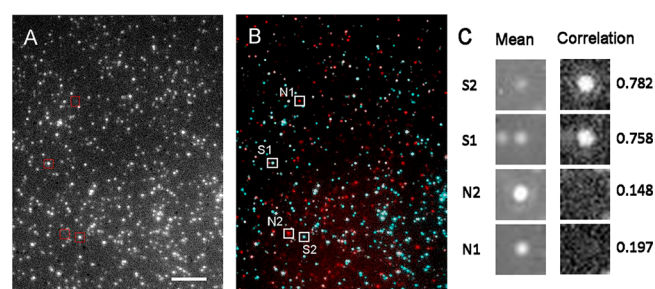


**Figure 4.** OLID imaging of a mixture of Cy3/5DNA and Cy5DNA immobilized on a polylysine-coated coverglass. (A) Correlation image (scale bar  $5 \mu\text{m}$ ). (B) Overlay of correlation image (blue) and mean image of the 200-frame movie (red), which reflects a color-coded map of switching and nonswitching molecules, respectively. (C) Zoom of the boxed areas in (B): comparison of mean and correlation images, and correlation coefficients of the central pixel of each box.

between the correlation image (blue) and the mean image of the 200 frames (red), and represents a color-coded map in which photoswitchable molecules (Cy3/5DNA) appear in blue and nonphotoswitchable molecules (Cy5DNA) in red. Two-thirds of the molecules appear as blue in the overlaid image, consistent with the sample composition. Four representative examples are shown in Figure 4C, for which the mean and correlation images are shown as well as the correlation coefficients. Molecules S1 and S2 are faint in the mean image, suggesting that they did not fluoresce for significant time during the experiment. However, they appear as bright spots in the correlation image, consistent with high correlation values. This indicates that they reproduced well the photoswitching behavior of the reference waveform and can be assigned to Cy3/5DNA. The method can readily distinguish two molecules with different photoswitching behaviors that are close to each other, as seen in panel S1. The low correlation values in panels N1 and N2 suggest that these two molecules are Cy5DNA. The pixel intensity traces of these panels and their similarity with

the reference waveform are shown in Figure S3 in the Supporting Information.

## CONCLUSIONS

In conclusion, the unique properties of CyDNA can be exploited for a wide range of applications in fluorescence labeling.<sup>17</sup> We have studied the potentially detrimental effect of overlabeling on fluorescence emission, and we have shown that two different mechanisms, aggregate formation and RET, are responsible for fluorescence quenching at high labeling densities. While RET has a similar effect for both Cy3- and Cy5DNA, the formation of nonfluorescent H-aggregates in Cy5DNA results in higher overall quenching efficiency for this biopolymer.

On the other hand, we have been able to engineer CyDNA to perform reversible and reliable fluorescence photoswitching, which opens up a range of potential applications in super-resolution imaging. This novel DNA biopolymer, which combines high-density labeling and controllable fluorescence photoswitching, constitutes a new class of photoactive DNA-based nanomaterial.<sup>27,28</sup> The DNA scaffold, which is nuclease resistant,<sup>17</sup> provides a biocompatible and photoswitchable macromolecule that is of great interest for advanced microscopy of cellular components.<sup>29</sup> Moreover, sequence specificity in labeling, which is crucial for applications such as fluorescence in situ hybridization (FISH) and the study of chromosome structure,<sup>30</sup> can be achieved by using the appropriate template in PCR-mediated synthesis of CyDNA. Fluorescence photoswitching in CyDNA can greatly improve imaging of chromosome loci with advanced fluorescence microscopy methods such as OLID and super-resolution imaging in combination with FISH and fiber-FISH,<sup>31</sup> offering great potential for high-resolution cytogenetics.

## ASSOCIATED CONTENT

### Supporting Information

Materials and methods; fluorescence quenching quantification in Cy3- and Cy5DNA; PALM imaging; pixel values and reference waveform for OLID experiment. This material is available free of charge via the Internet at <http://pubs.acs.org>.

## AUTHOR INFORMATION

### Corresponding Author

\*E-mail: [cristina.flors@imdea.org](mailto:cristina.flors@imdea.org).

### Notes

The authors declare no competing financial interest.

## ACKNOWLEDGMENTS

This work has been funded by The Royal Society (UF090182, C.F.), the Spanish Ministerio de Economía y Competitividad (RYC-2011-07637, C.F.), and MRC program grant MC\_US\_A024\_0014 (P.H.). D.A.S. holds a Universitas 21 Joint Ph.D. Scholarship (University of Edinburgh/University of Melbourne). We thank John White for assistance with PCR and Peter Dedecker (Katholieke Universiteit Leuven, Belgium) for the Localizer software for data analysis.

## REFERENCES

(1) Hell, S. W. *Nat. Methods* **2009**, *6* (1), 24–32.  
(2) Heilemann, M.; Dedecker, P.; Hofkens, J.; Sauer, M. *Laser Photonics Rev.* **2009**, *3* (1–2), 180–202.

(3) Tian, Z. Y.; Wu, W. W.; Li, A. D. Q. *Chemphyschem* **2009**, *10* (15), 2577–2591.  
(4) Cusido, J.; Impellizzeri, S.; Raymo, F. M. *Nanoscale* **2011**, *3* (1), 59–70.  
(5) Marriott, G.; Mao, S.; Sakata, T.; Ran, J.; Jackson, D. K.; Petchprayoon, C.; Gomez, T. J.; Warp, E.; Tulyathan, O.; Aaron, H. L.; Isacoff, E. Y.; Yan, Y. L. *Proc. Natl. Acad. Sci. U.S.A.* **2008**, *105* (46), 17789–17794.  
(6) Yan, Y. L.; Marriott, M. E.; Petchprayoon, C.; Marriott, G. *Biochem. J.* **2011**, *433*, 411–422.  
(7) van de Linde, S.; Wolter, S.; Heilemann, M.; Sauer, M. *J. Biotechnol.* **2010**, *149* (4), 260–6.  
(8) Shroff, H.; Galbraith, C. G.; Galbraith, J. A.; Betzig, E. *Nat. Methods* **2008**, *5* (5), 417–23.  
(9) Cordes, T.; Strackharn, M.; Stahl, S. W.; Summerer, W.; Steinhauer, C.; Forthmann, C.; Puchner, E. M.; Vogelsang, J.; Gaub, H. E.; Tinnefeld, P. *Nano Lett.* **2010**, *10*, 645–51.  
(10) Flors, C. *Biopolymers* **2011**, *95*, 290–297.  
(11) Flors, C.; Ravarani, C. N. J.; Dryden, D. T. F. *Chemphyschem* **2009**, *10* (13), 2201–4.  
(12) Flors, C. *Photochem. Photobiol. Sci.* **2010**, *9* (5), 643–8.  
(13) Schoen, I.; Ries, J.; Klotzsch, E.; Ewers, H.; Vogel, V. *Nano Lett.* **2011**, *11*, 4008–11.  
(14) Jungmann, R.; Steinhauer, C.; Scheible, M.; Kuzyk, A.; Tinnefeld, P.; Simmel, F. C. *Nano Lett.* **2010**, *10* (11), 4756–61.  
(15) Benke, A.; Manley, S. *Chembiochem* **2012**, *13* (2), 298–301.  
(16) Zessin, P. J.; Finan, K.; Heilemann, M. *J. Struct. Biol.* **2012**, *177* (2), 344–8.  
(17) Ramsay, N.; Jemth, A. S.; Brown, A.; Crampton, N.; Dear, P.; Holliger, P. *J. Am. Chem. Soc.* **2010**, *132*, 5096–104.  
(18) Bates, M.; Blosser, T. R.; Zhuang, X. W. *Phys. Rev. Lett.* **2005**, *94* (10), 108101.  
(19) Conley, N. R.; Biteen, J. S.; Moerner, W. E. *J. Phys. Chem. B* **2008**, *112*, 11878–80.  
(20) Herz, A. H. *Photogr. Sci. Eng.* **1974**, *18* (3), 323–335.  
(21) Randolph, J. B.; Waggoner, A. S. *Nucleic Acids Res.* **1997**, *25* (14), 2923–9.  
(22) Kang, J.; Kaczmarek, O.; Liebscher, J.; Daehne, L. *Int. J. Polym. Sci.* **2010**, *2010*, article ID 264781.  
(23) Gruber, H. J.; Hahn, C. D.; Kada, G.; Riener, C. K.; Harms, G. S.; Ahrer, W.; Dax, T. G.; Knaus, H. G. *Bioconjugate Chem.* **2000**, *11* (1), 696–704.  
(24) Luchowski, R.; Matveeva, E. G.; Gryczynski, I.; Terpetschnig, E. A.; Patsenker, L.; Laczko, G.; Borejdo, J.; Gryczynski, Z. *Curr. Pharm. Biotechnol.* **2008**, *9* (5), 411–20.  
(25) Dempsey, G. T.; Bates, M.; Kowtoniuk, W. E.; Liu, D. R.; Tsien, R. Y.; Zhuang, X. *J. Am. Chem. Soc.* **2009**, *131*, 18192–3.  
(26) Heilemann, M.; Margeat, E.; Kasper, R.; Sauer, M.; Tinnefeld, P. *J. Am. Chem. Soc.* **2005**, *127*, 3801–3806.  
(27) Varghese, R.; Wagenknecht, H. A. *Chem. Commun. (Cambridge)* **2009**, *19*, 2615–24.  
(28) Teo, Y. N.; Kool, E. T. *Chem. Rev.* **2012**, *112* (7), 4221–45.  
(29) Yildiz, I.; Impellizzeri, S.; Deniz, E.; McCaughan, B.; Callan, J. F.; Raymo, F. M. *J. Am. Chem. Soc.* **2011**, *133*, 871–9.  
(30) Flors, C.; Earnshaw, W. C. *Curr. Opin. Chem. Biol.* **2011**, *15* (6), 838–44.  
(31) Markaki, Y.; Smeets, D.; Fiedler, S.; Schmid, V. J.; Schermelleh, L.; Cremer, T.; Cremer, M. *Bioessays* **2012**, *34* (5), 412–26.